ORIGINAL ARTICLE DOI: 10.20515/otd.1772344

Osmangazi Journal of Med, 2026;48(4):590-607

Osmangazi Journal of Medicine

e-ISSN: 2587-1579

Biochemical and Histological Evaluation of The Impacts of Conivaptan and Boric Acid on Ischemia-induced Tissue Injury

Konivaptan ve Borik Asidin İskemi Kaynaklı Doku Hasarı Üzerindeki Etkilerinin Biyokimyasal ve Histolojik Açıdan Değerlendirilmesi

Betül Can[1], Fatih Kar[2], Ezgi Kar[3], Mete Özkoç[4], Hakan Şentürk[5], Dilek Burukoğlu Dönmez[6], Güngör Kanbak[1], Ibrahim Özkan Alataş[1]

[1] Eskisehir Osmangazi University, Faculty of Medicine, Department of Medical Biochemistry, Eskisehir, Türkiye
[2] Kutahya Health Sciences University, Faculty of Medicine, Department of Medical Biochemistry, Kutahya, Türkiye
[3] Kutahya Health Sciences University, Faculty of Health Sciences, Department of Nutrition and Dietetics, Kutahya, Türkiye
[4] University of Kyrenia, Faculty of Medicine, Department of Medical Biochemistry, North Cyprus, Mersin 10, Türkiye
[5] Eskisehir Osmangazi University, Faculty of Science, Department of General Biology, Eskisehir, Türkiye
[6] Eskisehir Osmangazi University, Faculty of Medicine, Department of Histology and Embryology, Eskisehir, Türkiye

Correspondence / Sorumlu yazar
Betül CAN

Eskisehir Osmangazi University, Faculty of Medicine, Department of Medical Biochemistry, Eskisehir, Türkiye

e-mail: betul_cn@yahoo.com

Received : 26.08.2025

Accepted : 23.03.2026

Abstract: Ischemia-reperfusion (I/R) injury, which is a major cause of acute kidney injury (AKI), involves complicated pathophysiological process triggered by oxidative and inflammatory mechanisms. This process adversely affects kidneys and distant organs/systems, potentially leading to multiple organ failure. Therefore, experimental studies targeting renal I/R injury mechanisms are needed to mitigate local and distant organ damage. We established an experimental renal I/R rat model to mimic the clinical presentation of AKI and evaluated the potential damage-preventive effects of conivaptan (CON) and boric acid (BA) on kidneys and distant tissues (liver, brain, heart, pancreas, testis, spleen). Accordingly, rats were divided into the groups: Control (sham-operated), Ischemia–reperfusion (I/R), I/R + Dimethyl sulfoxide (I/R + DMSO) I/R + Conivaptan (I/R + CON), and I/R + Conivaptan + Boric acid (I/R + CON + BA). TAS, TOS, and total thiol levels, which indicated oxidant and antioxidant redox status, were measured in blood samples, and the oxidative stress index was calculated. Inflammation-related cytokines (TNF-α, interleukin (IL)-6, IL-10, IL-35, and chemerin) were analysed through ELISA and/or RT-PCR. Furthermore, serum enzyme activities, lipid-profile, and albumin levels were determined. Tissue samples were examined histologically using Hematoxylin-Eosin staining. Renal I/R injury significantly increased systemic oxidative stress, exacerbated renal inflammation, and induced distant organ damage. Treatment with CON and BA demonstrated protective effects by reducing oxidative stress and modulating inflammatory responses without inducing toxicity in the postischemic period. Our findings suggest that CON and BA exhibit anti-inflammatory and antioxidant properties in the early phase of postischemic injury process and may be effective in attenuating distant organ damage following renal I/R injury.

Keywords: Boric acid, Conivaptan, Inflammation, Acute kidney injury, Ischemia-reperfusion, Oxidative stress

Özet: Akut böbrek hasarının (ABH) başlıca nedenlerinden biri olan iskemi-reperfüzyon (İ/R) hasarı, oksidatif ve inflamatuar mekanizmaların tetiklendiği kompleks patofizyolojik süreçleri içermektedir. Bu süreçler, böbrek ve uzak organ/sistemleri olumsuz etkileyerek çoklu organ yetmezliğine yol açabilmektedir. Bu nedenle, lokal ve uzak organ hasarını azaltmaya yönelik, böbrek İ/R hasarı mekanizmalarını hedef alan deneysel çalışmaların planlanması önemli bir ihtiyaçtır. Bu çalışmada, ABH kliniğini yansıtmak için deneysel bir böbrek İ/R sıçan modeli oluşturulmuştur; konivaptan (CON) ve borik asidin (BA) böbrekler ve uzak dokular (karaciğer, beyin, kalp, pankreas, testis, dalak) üzerindeki potansiyel hasar önleyici etkileri araştırılmıştır. Buna göre, sıçanlar Kontrol (sham-opere), İskemi-reperfüzyon (I/R), I/R + Dimetilsülfoksit (I/R + DMSO), I/R + Konivaptan (I/R + CON) ve I/R + Konivaptan + Borik asit (I/R + CON + BA) olmak üzere gruplara ayrılmıştır. Oksidan ve antioksidan redoks durumunu gösteren TAS, TOS ve total tiyol düzeyleri kan örneklerinde ölçülmüştür ve oksidatif stres indeksi hesaplanmıştır. İnflamasyonla ilişkili sitokinler (TNF-α, interlökin (IL)-6, IL-10, IL-35 ve kemerin) ELISA ve/veya RT-PCR ile analiz edilmiştir. Ayrıca, serum enzim aktiviteleri, lipit profili ve albümin düzeyleri belirlenmiştir. Doku örnekleri Hematoksilen-Eozin boyama kullanılarak histolojik olarak incelenmiştir. Çalışmamızda böbrek I/R hasarının sistemik oksidatif stresi önemli ölçüde artırdığı, böbrek inflamasyonunu şiddetlendirdiği ve uzak organ hasarını indüklediği gözlenmiştir. CON ve BA tedavisi, iskemi sonrası dönemde toksisiteye neden olmadan oksidatif stresi azaltarak ve inflamasyon yanıtlarını düzenleyerek koruyucu etki göstermiştir. Bulgularımız, CON ve BA'nın iskemi sonrası hasar sürecinin erken evresinde anti-inflamatuar ve antioksidan özellikler gösterdiğini ve böbrek I/R hasarını takiben uzak organ hasarını hafifletmede etkili olabileceğini destekler niteliktedir.

Anahtar Kelimeler: Borik asit, Konivaptan, İnflamasyon, Akut böbrek hasarı, İskemi-reperfüzyon, Oksidatif stres

Ethics Committee Approval: The study was approved by the Eskisehir Osmangazi University Animal Experiments Local Ethics Committee (Decision No: 772, Date: 10.10.2019).

Informed Consent: The authors state that informed consent was not applicable due to the nature of the study.

Authorship Contributions: Concept: BC, FK, HŞ. Surgical Practices: HŞ, BC, FK, EK, MO. Biochemical Analysis and Interpretation: HŞ, BC, FK, EK, MO, GK, İOA. Histological Analysis and Interpretation: DBD. Literature Search: BC. Writing: BC.

Copyright Transfer Form: Copyright Transfer Form was signed by all authors.

Peer-review: Internally peer-reviewed.

Conflict of Interest: No conflict of interest was declared by the authors.

Financial Disclosure: This study contains previously unpublished results of the project, which was financially supported by the Scientific Research Projects Commission of the Eskisehir Osmangazi University (Eskisehir, Turkey) (Project #202011011). A part of this study was presented at the International Laboratory Medicine and XXth National Clinical Biochemistry Congress held on 25-26 December 2020.

How to cite/ Atıf için: Can B, Kar F, Kar K, Özkoç M, Şentürk H, Burukoğlu Dönmez D, Kanbak G, Alataş IO, Biochemical and Histological Evaluation of The Impacts of Conivaptan and Boric Acid on Ischemia-induced Tissue Injury, Osmangazi Journal of Medicine, 2026;48(4):590-607

1. Introduction

Acute kidney injury (AKI) is a common clinical syndrome with a broad spectrum of crucial pathophysiological processes, which affect the renal structure as characterized by an instantaneous decrease in renal function (1, 2). AKI can occur as a major complication in 10%–15% of all hospitalized patients, and the prevalence of AKI can sometimes exceed 50%, especially in intensive care unit patients (3, 4). It was suggested that AKI had a poor outcome in hospitalized critically ill patients, and nearly 2 million patients die each year in the world because of AKI (5).

The pathophysiology of renal injury caused by ischemia-reperfusion (I/R), as a prevalent reason of AKI, involves complicated processes, in which oxidative and inflammatory pathways are triggered, that not only damage the kidney but also affect distant organs/systems, including lung, liver, heart, intestine, brain, pancreas, and hematological system (6,7). Despite extensive research, effective therapeutic strategies to mitigate both local and systemic consequences of I/R injury remain limited. Therefore, experimental models simulating human AKI are essential for evaluating potential interventions. Various experimental models with different properties depending on the method of induction, including septic (e.g., induced by lipopolysaccharide injection or caecal ligation) or aseptic (e.g., induced by I/R injury or nephrotoxic substances) have been developed and characterized to understand the pathophysiological mechanisms of human renal diseases associated with these processes and investigate the therapeutic efficacy of various agents (8-10). Among aseptic models, the rodent models, which find frequent use, include surgery-based bilateral, unilateral, bilateral, and contralateral nephrectomy with unilateral I/R injuries (11-13). In particular, the contralateral nephrectomy with unilateral I/R model is widely preferred to represent kidney injury in humans (14,15).

Antidiuretic hormone (ADH), a potent endogenous antidiuretic, has an important functional role in fluid homeostasis. Nevertheless, it was suggested that high ADH levels in animal and human models might be related with the pathogenesis/progression of several kidney diseases (16). Conivaptan (CON), a benzozapine derivative, is an ADH receptor antagonist. CON is approved by the FDA for the intravenous treatment of patients with euvolemic and hypervolemic hyponatremia and has an electrolyte-sparing aquaresis effect (17,18). It is available in oral or intravenous forms, but intravenously administered forms are preferred in treatment due to the drug interaction potential associated with cytochrome P-450 enzyme inhibition (19). Previous studies reported that the expansion of renal functional alterations was prevented by CON, especially by blocking of V_{1a} and V_2 ADH receptors (20). Nevertheless, there is quite limited investigation on the relation between CON and inflammatory and oxidative damage processes in cases of AKI.

Boron is a semiconductor metalloid. Boron is found in nature as a constituent of boric acid (BA), borax, borates, ulexite, and colemanite because of boron's propensity to bind to electron-rich elements (such as C, N and O) (21). Today, boron and its compounds have more than 250 uses in the nuclear, aerospace, chemical, cosmetics, energy, pharmaceutical, and healthcare industries (22). Upon experimental studies in the field of health, it was reported that boron compounds could have various pleiotropic effects, including anti-inflammatory (23), antioxidant (24), anticarcinogenic (25), antiosteoporotic (26), antimicrobial (27), and even antiviral efficiency (28) depending on the dose applied. These effects were suggested by different experimental disease models, including fetal alcohol syndrome (29), traumatic brain injury (30), prostate cancer (31), myocardial infarction (32), I/R injury (15), ulcerative colitis (33), and acute alcohol-induced tissue injury (34). Given that BA can react with several functional groups such as alcohol, carboxylic, thiol, or amine groups, it can change the physical and chemical stability of any molecule in a positive or negative direction (35). It is also important to consider this detail when investigating the therapeutic effects of BA.

Given this background, the present study aimed to investigate the efficiency of CON and BA, administered at the onset of reperfusion, on kidney and distant tissues, including liver, brain, heart, pancreas, testis, and spleen, in an established rodent model of AKI. By combining biochemical, molecular, and histological analyses, this study seeks to fill a critical gap in understanding the potential synergistic roles of these agents in ameliorating I/R-induced tissue damage.

2. Materials and Methods

2.1. Animals and Study Design

All animal experiments were performed at Medical and Surgical Experimental Animals Application and Research Center of the Eskisehir Osmangazi University. Accordingly, 40 Sprague–Dawley rats (3-4 months of age, weighing 250–300 g, males) were housed in a humidity-controlled environment at ambient temperature for 12 hours a day and 12 hours at night in this center before the experiments. The experimental research protocol was carried out pursuant to the principles stated in the Declaration of Helsinki and upon permission of the Local Ethics Committee of the University for Animal Experiments (Protocol #772/2019).

The study design is illustrated in Figure 1. Male Sprague–Dawley rats were assigned into 5 groups at random, with 8 rats per group. The groups were constituted as detailed below:

- Control Group: Unilateral nephrectomy (no ischemia)
- I/R Group: Unilateral nephrectomy, 45 min ischemia, and reperfusion
- I/R + Dimethyl sulfoxide (DMSO) Group (I/R + DMSO): Unilateral nephrectomy, 45 min ischemia, 5% DMSO (i.v.) at reperfusion onset
- I/R + CON Group: Unilateral nephrectomy, 45 min ischemia, 10 mg/mL/kg CON (i.v) at reperfusion onset
- I/R + CON + BA Group: Unilateral nephrectomy, 45 min ischemia, 10 mg/mL/kg CON (i.v) and 50 mg/kg BA (i.p) at reperfusion onset

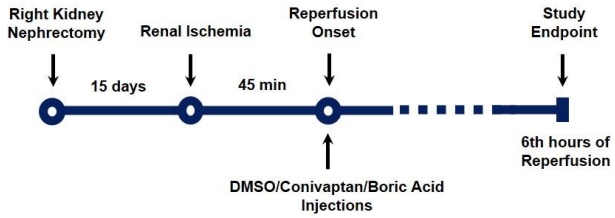

Figure 1. *Study design and experimental timeline*

The AKI model was established based on previously described protocol (14). In brief, all experimental groups underwent right kidney nephrectomy to establish this model. Upon a 15-day recovery period, ischemia was performed by occlusion of the left renal pedicle with the help of a vascular clamp under anesthesia (ischemia was not performed in the control group). Furthermore, 5% DMSO (i.v.) (cat. #D5879, Sigma-Aldrich, USA), 10 mg/mL/kg CON (i.v.; in 5% final DMSO) (cat. #TRC-C384700, Toronto Reasarch Chemicals, Canada), and 50 mg/kg BA (i.p.; in saline) (cat. #A2940, AppliChem GmbH, Germany) were administered to the respective groups at the onset of reperfusion. Dimethyl sulphoxide is often used as a solvent in both *in vivo* and *in vitro* pharmacological research to enhance the solubility (and penetrability) of many poorly soluble hydrophobic molecules (36,37). It was used in this study to dissolve conivaptan before intravenous administration.

The CON and BA doses or application periods were based upon previous studies (38,39). The vascular clamps were released to confirm renal reperfusion after the administration of the corresponding treatments, and the incision sites were sutured. To prevent hypovolemia, sterile saline solution was administered intraperitoneally. Six hours after reperfusion (contemporaneously for the control), cardiac blood and tissue samples (kidney, liver, brain, heart, pancreas, testis, and spleen) were collected under anesthesia. Serum was isolated by centrifugation (1000 × g, 10 min). Kidney tissues were kept in refrigerator at -80°C for further analyses. Liver, brain, heart, pancreas, testis, and spleen were fixed in 10% neutral buffered formalin for subsequent histological assessments.

2.2 Tests on Serum Samples

Alanine aminotransferase (ALT), aspartate aminotransferase (AST), alkaline phosphatase (ALP), and lactate dehydrogenase (LDH) activity, as well as lipid profile (total cholesterol, LDL, HDL, and triglyceride) and albumin levels, were evaluated in rat serum samples using Roche Cobas c702 analyser using commercial test kits. Enzyme activity results were expressed as U/L, albumin levels as g/dL, and lipid levels as mg/dL.

Total antioxidant status (TAS) (ref. #RL0017), total oxidant status (TOS) (ref. #RL0024), and total thiol levels (ref. #RL0178), which indicated oxidant and antioxidant redox status, were measured using test kits (Rel Assay Diagnostics, Turkey). Oxidative stress index (OSI), as an indicator of oxidative load, was assessed by an equation in the manner described hereafter (40):

OSI (Arbitrary Unit) = (TOS, μmol H_2O_2eq/L) / (TAS, mmol Trolox eq/L)

Additionally, serum levels of TNF-α (cat. #E-EL-R0019, Elabscience, USA) (41), interleukin-6 (IL-6) (cat. #E-EL-R0015, Elabscience, USA) (41), IL-10 (cat. #E-EL-R0016, Elabscience, USA) (42), IL-35 (cat. #E2118Ra, BT LAB, China) (33), and chemerin (cat. #E0864Ra, BT LAB, China) (43) were measured using a BioTek ELx800 Microplate reader and commercial ELISA kits to examine cytokine levels representative of the inflammatory status. TNF-α, IL-6, and IL-10 levels were given as pg/mL, and IL-35 ng/L and chemerin levels were expressed as ng/dL.

2.3. Real-time PCR (QPCR) Analysis of Kidney Tissue

TNF-α, IL-6, IL-10 and chemerin mRNA expressions were analysed through qPCR in kidney tissue samples. For this purpose, RNA isolation was performed following the kit protocol (cat. #BS88136, Bio Basic Inc., Canada). After the isolation, the amount of RNA in the samples was measured on a fluorometer using a test kit (ref. #Q32852, Invitrogen, Thermo Fischer Scientific, UK). After the samples were treated in accordance with the kit (cat. #C03-01-05, A.B.T, Turkey), the reaction was set up in the SimpliAmp Thermal Cycler (Applied biosystems, Thermo Fischer) in accordance with the cDNA Data Sheet. As a result of the reaction, cDNA samples of each rat in the experimental groups were obtained and kept at -20 ºC.

Stock primer solutions of 100 µM were prepared using nuclease-free water for β-actin (control gene), TNF-α, IL-6, IL-10, and Chemerin for qPCR analysis, each of the forward and reverse primers in lyophilized forms, in the volumes specified in the user manuals (Sentebiolab, Turkey). During the study, stock primer solutions were diluted 1:10 before used. The forward or reverse primer sequences used in the PCR reaction were shared in Table 1. mRNA expressions of TNF-α, IL-6, IL-10, and Chemerin were analysed in cDNA samples by Real-Time PCR with the relevant primers and SYBR Green Master Mix (cat. #Q03-02-01, A.B.T, Turkey). mRNA expression levels of TNF-α, IL-6, IL-10, and chemerin were normalized to β-actin and calculated using the $2^{-\Delta\Delta Ct}$ method (44). Primer sequences are listed in Table 1.

Table 1. Primers and primer sequences used in real-time PCR analysis

Primer name	Forward and reverse primer sequences (5′- 3′)	Length (bp)
TNF-α	F: CAT CCG TTC TCT ACC CAG CC	20
	R: AAT TCT GAG CCC GGA GTT GG	20
Interleukin-6	F: TCT GGT CTT CTG GAG TTC CGT	21
	R: GGA AGT TGG GGT AGG AAG GAC	21
Interleukin-10	F: TTG AAC CAC CCG GCA TCT AC	20
	R: CCA AGG AGT TGC TCC CGT TA	20
Chemerin	F: ACC ACA CAG AAA AGG GCC TC	20
	R: CTC TGT CCC GTG TAT GTC CG	20
β-actin (Housekeeping gene)	F: AGC CAT GTA CGT AGC CAT CC	20
	R: CTC TCA GCT GTG GTG GTG AA	20

2.4. Histological Analyses of the Tissues

Liver, brain, heart, pancreas, testis, and spleen tissues were placed in tissue tracking cassettes and preserved in 10% buffered neutral formaldehyde for histologic examination. Tissues were exposed to dehydration by treating with ethyl alcohol series, made transparent by xylol application and blocked in 3 different paraffins at 60°C oven for 30, 60, and 60 minutes, respectively. The microtome blade and other materials for standard hematoxylin–eosin (HE) staining of these blocks was cooled at −20°C the previous night. Furthermore, 5-µm-thick sections were collected by a microtome, paraffin-opened in a water bath, and covered on poly-L-lysine coated slides. They were left at 37°C overnight and deparaffinized in xylol. They were hydrated in a series of decreasing levels of ethyl alcohol followed by HE staining (45). All tissue sections were made permanent preserved preparations by using entellan and they were examined under an Olympus CH40 light microscope. The tissue histopathological features were evaluated by scoring from 0-3 (damage status, zero: none, one: mild, two: moderate, three: severe).

2.5. Statistical Analysis

The analyses were achieved via the GraphPad Prism version 8. The data distribution was evaluated by Shapiro–Wilk test. Comparisons for normal distributed variables were assessed using the one-way ANOVA followed by Tukey's post hoc test. The comparisons of variables that do not show Gaussian distribution were analysed by the Kruskal-Wallis test. Categorical data (histological scores) were analysed using Pearson's Chi-square test by Monte Carlo method for categorical variables. $p<0.05$ was described as significant.

3. Results

3.1. Serum ALT, AST, ALP, LDH, albumin, and lipids

Based on the results of statistical analysis of enzyme activity measurements, ALT and AST activities, as related to the liver function, tended to be elevated in all I/R groups, while ALP activity inclined to increase in I/R group and decrease in the others. Nevertheless, no significant intergroup difference in serum ALT, AST, and ALP activities was determined (Table 2). Upon analysis of the LDH activity, there were significant increases in all groups with reference to control, while there was a significant decrease in its activity, especially in I/R+CON+BA group with reference to I/R+CON group ($p<0.01$) (Table 2). Albumin levels decreased in I/R+DMSO group, and had a tendency to decrease in treatment groups (Table 2).

According to the serum lipid profile results, total cholesterol levels in I/R group were close to control (Table 2). Although total cholesterol levels tended to increase in treatment groups with reference to control and I/R groups, there was no important difference. The highest mean value was seen in I/R+DMSO group. Similar to total cholesterol, LDL-cholesterol levels decreased in I/R group, while the highest values were seen in I/R+DMSO group (Table 2). CON treatment decreased LDL-cholesterol levels, whereas combined treatment with BA was associated with an increase with reference to I/R group ($p<0.05$) (Table 2). HDL-cholesterol level tended to decrease in I/R+CON group, but it was a higher in I/R+CON+BA group than the I/R group ($p<0.05$) (Table 2). In contrast, triglyceride levels increased in I/R+CON group, whereas there was a significant decrease in I/R+CON+BA group with reference to I/R and I/R+CON groups ($p<0.01$) (Table 2).

Table 2. Statistical findings on serum enzyme activites, albumin and lipid profile tests in renal ischemia–reperfusion injury

Parameters / Groups	**Control (n=8)**	**I/R (n=8)**	**I/R+DMSO (n=8)**	**I/R+CON (n=8)**	**I/R+CON+BA (n=8)**	***p* values**
ALT (U/L)	93.5±11.15	106.3±23.37	97.6±11.28	107.8±5.742	101.6±7.702	ns*
AST (U/L)	385.5 (378.8-409.8)	398.6 (341.3-481.8)	396.6 (378.3-409.7)	438.8 (417.8-448)	398.3 (315.9-457.3)	ns**
ALP (U/L)	171±26.48	188.3± 8.61	170.5±38.44	168.4±8.986	158.8±16.32	ns*
LDH (U/L)	444.3 (402-598.6)	671 (636-720.3)	740 (725-759.5)[a]	978.2 (732.1-1171)[a]	597.8 (526-688)[d]	<0.01**
Albumin (g/dL)	3.6 (3.518-3.6)	3.6 (3.439-3.675)	3.367 (3.3-3.4) [a,b]	3.4 (3.325-3.475)	3.45 (3.4-3.5)	<0.05**
Total-cholesterol (mg/dL)	47.71±4.651	46.14±4.823	55±4.899[b]	49.6±3.005	52.33±7.244	<0.05*
LDL-cholesterol (mg/dL)	8.929 (7.25-10)	7.214 (6.25-8.75)	9.917 (9.208-11)[b]	8.1 (8-8.2)	9.333 (9-9.917)[b]	<0.05**
HDL-cholesterol (mg/dL)	39±3.625	37.38±4.719	37.38±5.706	34.88±3.137	42.75±5.175[d]	<0.05*
Triglyceride (mg/dL)	43.5 (33.75-48.5)	48.43 (41-54)	44.3 (34-45.6)	53.2 (41.8-61.75)	23.92 (21.5-26.46)[b,d]	<0.01**

** One-way analysis of variance test (mean ± standard deviation)*
*** Kruskal–Wallis test (median, Q25 and Q75 values)*
[a,b,c,d] Significant difference versus control, I/R, I/R + DMSO, and I/R + CON, respectively.
n, sample size; ns, not significant; I/R, ischemia-reperfusion, CON, conivaptan, BA, boric acid.

3.2. Serum TAS, TOS, and Total Thiol Levels

In the present study, TAS and TOS levels indicating oxidant and antioxidant redox status and total thiol levels were measured in rat serum samples, and OSI was calculated. Based on the results of statistical analysis, TAS levels were measured as 0.958±0.032 mmol Trolox eq/L in the control, whereas it was significantly increased in I/R+DMSO group with a value of 1.152±0.173 mmol with reference to control (Figure 2a). Similarly, TAS levels increased in I/R+CON group (1.180 ± 0.059 mmol Trolox eq/L) and I/R+CON+BA group (1.173 ± 0.075 mmol Trolox eq/L) with reference to the control ($p< 0.01$). TOS levels were 7.308 ± 0.799 μmol H_2O_2 eq/L in control, and increased in I/R+DMSO group (9.455 ± 1.252 μmol H_2O_2 eq/L) ($p< 0.01$) (Figure 2b). Furthermore, TOS levels were significantly decreased with 7.40 ± 1.007 μmol H_2O_2eq/L in I/R+CON group compared to IR+DMSO group ($p< 0.05$). Similarly, TOS levels were lower in I/R+CON+BA group (7.253 ± 0.992 μmol H_2O_2) with reference to IR+DMSO group ($p < 0.01$). In contrast, there was no intergroup difference in total thiol levels ($p> 0.05$) (Figure 2c). OSI levels increased slightly from 7.625 ± 0.773 arbitrary units in control to 8.282±1.104 in IR+DMSO group, albeit this change was not significant ($p> 0.05$) (Figure 2d). In contrast, a significant decrease was recognized in I/R+CON group (6.26 ± 0.680 arbitrary units) and I/R+CON+BA group (6.239 ± 1.207 arbitrary units) with reference to IR+DMSO group ($p< 0.01$) (Figure 2d). These results regarding TAS, TOS, and OSI values supported that CON alone or combined with BA was positively effective against oxidative stress caused by renal I/R injury.

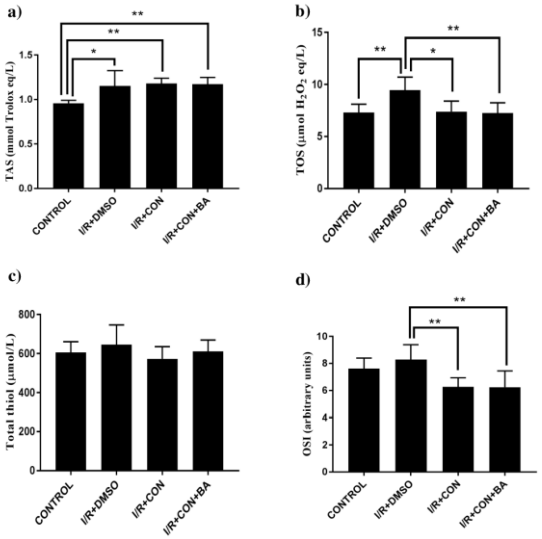

Figure 2*. Serum oxidative stress markers in rats subjected to renal ischemia-reperfusion (I/R) injury (n=8 per group). (a) Total antioxidant status (TAS), (b) total oxidant status (TOS), (c) total thiol levels, and (d) oxidative stress index (OSI) in serum samples. Intergroup differences are demonstrated with lines and via * or ** for significance at p <0.05 and p <0.01, respectively. I/R, ischemia-reperfusion; DMSO, dimethyl sulfoxide; CON, conivaptan; BA, boric acid.*

3.3. Serum TNF-α, IL-6, IL-10, IL-35, and Chemerin Levels

Proinflammatory cytokines TNF-α and IL-6, anti-inflammatory IL-10, anti-inflammatory and immunosuppressive IL-35, and chemerin, an adipocytokine that recently came to the forefront in kidney diseases, were determined in serum samples to research the effects of CON and BA on inflammatory processes in acute ischemic kidney injury. Based on the results of statistical analysis, proinflammatory TNF-α levels increased in I/R+DMSO group with reference to control group ($p< 0.05$), while there was no significant difference among the other groups (Table 3). There was no important intergroup difference in IL-6 levels (Table 3). It was seen that anti-inflammatory IL-10 was the highest levels in I/R+CON group ($p< 0.0001$) (Table 3). Although IL-35 and chemerin levels tended to increase in treatment groups, there was no significant intergroup difference (Table 3). These results show that CON and its combination with BA prevented the exacerbation of systemic inflammation in the early postischemic period and sought to keep it under control, but the absence of serious

inflammation during this period made it difficult to understand the clear effect of these agents.

Table 3. Statistical findings on serum cytokine levels in renal ischemia–reperfusion injury

Parameters / Groups	Control (n=8)	I/R+DMSO (n=8)	I/R+CON (n=8)	I/R+CON+BA (n=8)	*p* values
TNF-α (pg/mL)	21.6 (21.6-22.11)	23.41 (22.93-24.26)[a]	22.07 (21.6-22.16)	22.68 (22.29-23.37)	<0.05**
Interleukin-6 (pg/mL)	7.223 (7.066-7.371)	7.103 (7.043-7.133)	7.205 (7.016-7.291)	7.163 (7.133-7.223)	ns**
Interleukin-10 (pg/mL)	3.653 (2.863-4.606)	6.071 (3.091-6.505)	15.88 (14.48-18.82)[a,b]	5.235 (4.082-6.309)[c]	<0.0001**
Interleukin-35 (ng/L)	74.21±25.18	85.58±23.16	99.84±24.7	100.9±25.78	ns*
Chemerin (ng/dL)	7.762±2.368	6.916±1.843	8.366±2.33	9.349±2.382	ns*

* One-way analysis of variance test (mean ± standard deviation)
** Kruskal–Wallis test (median, Q25 and Q75 values)
[a,b,c] Difference versus control, I/R+DMSO or I/R+CON groups, respectively.
n, sample size; ns, not significant (p>0.05); I/R, ischemia-reperfusion, CON, conivaptan, BA, boric acid.

3.4. TNF-α, IL-6, IL-10 and Chemerin Expression Levels in Kidney

Figure 3 shows the differences on qPCR results among the groups. TNF-α expression levels increased about 3-fold in I/R and I/R+DMSO groups with reference to control (Fig. 3a). IL-6 expression levels increased over 12-fold in these groups (p<0.0001) (Fig. 3b). TNF-α and IL-6 expression levels in I/R+CON and I/R+CON+BA groups have been found as lower than in I/R and I/R+DMSO groups (p<0.0001). Especially in I/R+CON+BA group, the expressions of these pro-inflammatory cytokines have been found to be closer to the control (p<0.0001) (Figure 3a, b). IL-10 and chemerin mRNA expression levels were lower in I/R+CON and I/R+CON+BA groups (Figure 3c, d). As a result, the renal I/R has triggered inflammatory processes in kidney tissue. Unlike our serum cytokine findings reflecting systemic inflammation, conivaptan and boric acid treatments have shown considerable anti-inflammatory effect in kidney during the early phases of renal injury process.

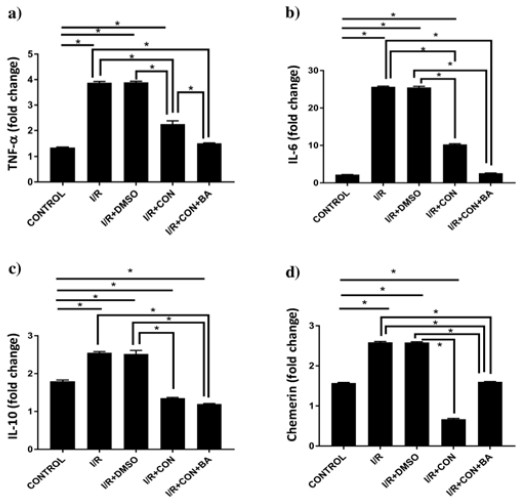

Figure 3*. Renal mRNA expression levels of cytokines in rats following I/R injury (n=8 per group). (a) Tumor necrosis factor-alpha (TNF-α), (b) interleukin-6 (IL-6), (c) interleukin-10 (IL-10) and (d) chemerin levels. Intergroup differences are pointed at connecting lines and by *p <0.0001. I/R, ischemia-reperfusion; DMSO, dimethyl sulfoxide; CON, conivaptan; BA, boric acid.*

3.5. Liver Tissue Histology

Upon microscopic examination of the rat liver tissue sections stained with HE, the liver appeared normal in the control group with euchromatic nucleated hepatocytes, sinusoidal structures, and vena centralis structures (Figure 4A) (Table 4). There were necrotic hepatocytes with pyknotic nuclei and eosinophilic cytoplasm in the parenchymal tissue and necrotic areas in periportal region, intravenular congestion, edema, and inflammation in the portal area in rat livers of I/R group (Figure 4B). In I/R+DMSO group, there were necrotic hepatocytes with pyknotic nuclei and eosinophilic cytoplasm, karyolysis, and vascular congestion in the parenchymal tissue (Figure 4C). Although minimal degeneration was seen in the pericentral cells of I/R+CON treatment group livers, there was reduced damage and near-normal liver structure (Figure 4D). However, there were a few hepatocytes with pyknotic nuclei in the parenchymal tissue, a near-normal structure with cells, sinusoidal structures, and vena centralis in I/R+CON+BA group (Figure 4E).

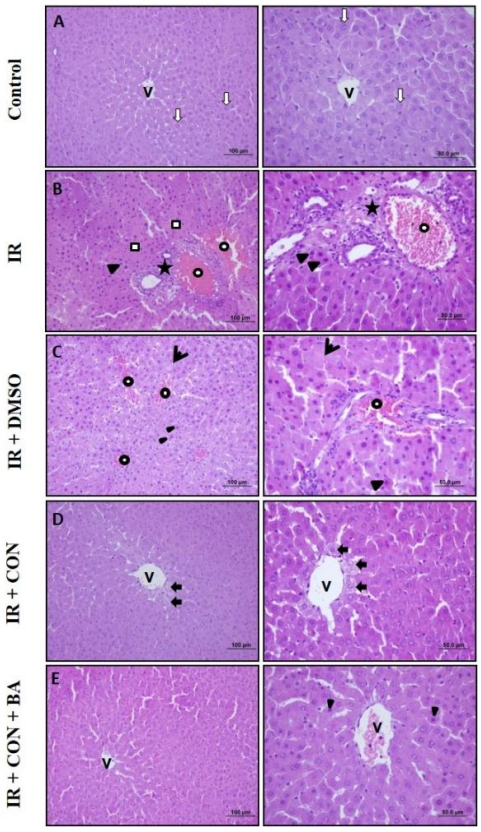

Figure 4. *Representative images of rat liver sections. (A) Liver structure with normal appearance, including hepatocyte cells with euchromatic nuclei (⇨), sinusoidal structures, and vena centralis (v) structures in the control group. (B) Necrotic hepatocyte cells with pyknotic nuclei and eosinophilic cytoplasm in parenchymal tissue (▶) and necrotic areas (□) in the periportal area, intravascular congestion (o), edema (★), and inflammation in the portal area in the ischemia/reperfusion (I/R) group. (C) Hepatocytes with pyknotic nuclei and eosinophilic cytoplasm (▶), karyolysis (→), and vascular congestion (o) in parenchyma tissue in DMSO group. (D) Minimal degeneration of pericentral cells (➡), reduced damage and near-normal liver structure in I/R+CON group livers. (E) Hepatocytes with a few pyknotic nuclei in the parenchyma (►) of I/R+CON+BA group; near-normal liver structure with sinusoidal and vena centralis (v) structures (Hematoxylin–eosin; scale bar: left to right 100µm, 50.0µm). I/R, ischemia-reperfusion; DMSO, dimethyl sulfoxide; CON, conivaptan; BA, boric acid.*

Table 4. Histological data of rat liver tissue sections in renal ischemia–reperfusion injury

Liver: Histopathological features	Damage criteria	Control (n=8)	I/R (n=8)	I/R+DMSO (n=8)	I/R+CON (n=8)	I/R+CON+BA (n=8)	P values*
Necrotic Cell	None	8 (100%)	0	0	4 (50%)	0	<0,001
	Mild	0	0	0	4 (50%)	6 (75%)	
	Moderate	0	0	4 (50%)	0	2 (25%)	
	Severe	0	8 (100%)	4 (50%)	0	0	
Karyolysis	None	8 (100%)	0	0	6 (75%)	3 (37,5%)	<0,001
	Mild	0	0	0	2 (25%)	5 (62,5%)	
	Moderate	0	6 (75%)	2 (25%)	0	0	
	Severe	0	2 (25%)	6 (75%)	0	0	
Cellular degeneration	None	8 (100%)	0	0	3 (37,5%)	5 (62,5%)	<0,001
	Mild	0	0	7 (87,5%)	5 (62,5%)	3 (37,5%)	
	Moderate	0	0	1 (12,5%)	0	0	
	Severe	0	8 (100%)	0	0	0	
Inflammation / Edema	None	8 (100%)	0	0	6 (75%)	3 (37,5%)	<0,001
	Mild	0	0	4 (50%)	2 (25%)	4 (50%)	
	Moderate	0	1 (12,5%)	4 (50%)	0	1 (12,5%)	
	Severe	0	7 (87,5%)	0	0	0	
Vascular Congestion	None	8 (100%)	0	0	4 (50%)	5 (62,5%)	<0,001
	Mild	0	0	0	3 (37,5%)	3 (37,5%)	
	Moderate	0	1 (12,5%)	7 (87,5%)	1 (12,5%)	0	
	Severe	0	7 (87,5%)	1 (12,5%)	0	0	

**Pearson's Chi-Square test by Monte Carlo method (% within groups)*

3.6. Brain Tissue Histology

Upon a microscopic analysis of HE-stained brain tissue sections, there were neurons and glial cells with a normal appearance in cortical area of control group rats (Figure 5A) (Supplemental Table 1). A perivascular damage, vascular congestion, and necrotic cell structures were observed in cortical area in I/R group (Figure 5B). Similar to I/R group, there were cortical damage, perivascular damage, and many necrotic cell structures in DMSO group of rat brains (Figure 5C). In rat brains of I/R+CON group, there was decreased damage in the cortical area with reference to I/R group; a few necrotic cells and perivascular damage were seen along with normal euchromatic neurons (Figure 5D). In I/R+CON+BA group, despite a few necrotic cells and perivascular damage in the cortical area, there was decreased damage with reference to the I/R group and neuronal structures similar to the control (Figure 5E).

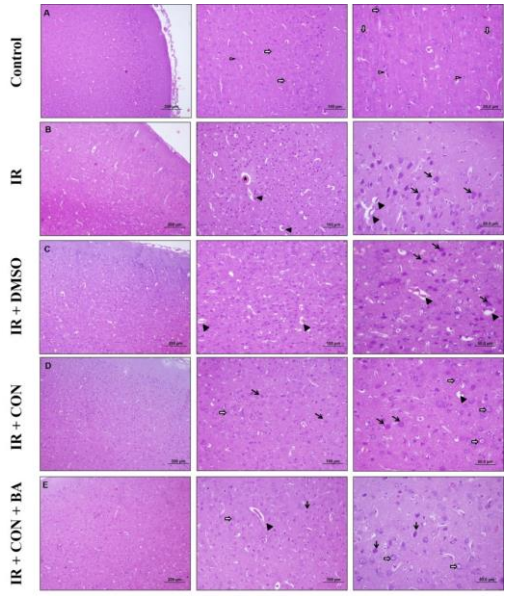

Figure 5. *Representative images of rat brain cortical sections. (A) Neurons (⇨) and glial cells (▷) with normal appearance in the cortical area in the control group. (B) Damage in the cortical area, perivascular damage (►), vascular congestion (★), and necrotic cellular structures (→) in the I/R group. (C) Cortical area damage, perivascular damage (►), and numerous necrotic cell structures (→) in the I/R+DMSO group. (D) Reduced damage in the cortical area in the I/R+CON group compared to the I/R group, few necrotic cells (→), and perivascular damage (►) along with normal euchromatic neurons (⇨). (E) In the I/R+CON+BA group, few necrotic cells (→) and perivascular damage (►) in the cortical area reduced damage compared to the I/R group, and neuronal structures (⇨) close to the control group (Hematoxylin–eosin; scale bar: left to right 200μm, 100μm, 50.0μm). I/R, ischemia-reperfusion; DMSO, dimethyl sulfoxide; CON, conivaptan; BA, boric acid.*

3.7. Heart Tissue Histology

Based on the HE staining results of rat heart tissue sections, histologically normal muscle cells with centrally located euchromatic nuclei were seen in control group; no cellular inflammation, edema, or necrosis was in this group (Figure 6A) (Supplemental Table 2). There were necrotic cells with pyknotic nuclei and eosinophilic cytoplasm, cellular inflammation, and vascular congestion in connective tissue of muscle fibers both in I/R and I/R+DMSO group (Figure 6B-6C). In I/R+CON group, there was reduced damage with reference to I/R group. However, with minimal cellular inflammation, the muscle cells with a histologic structure were close to normal with centrally located euchromatic nuclei (Figure 6D). In I/R+CON+BA group, the tissue damage was reduced with reference to I/R group; vascular congestion was seen in connective tissue of muscle fibers, but muscle cells were close to normal with centrally located euchromatic nuclei with reduced damage to the muscle cells (Figure 6E).

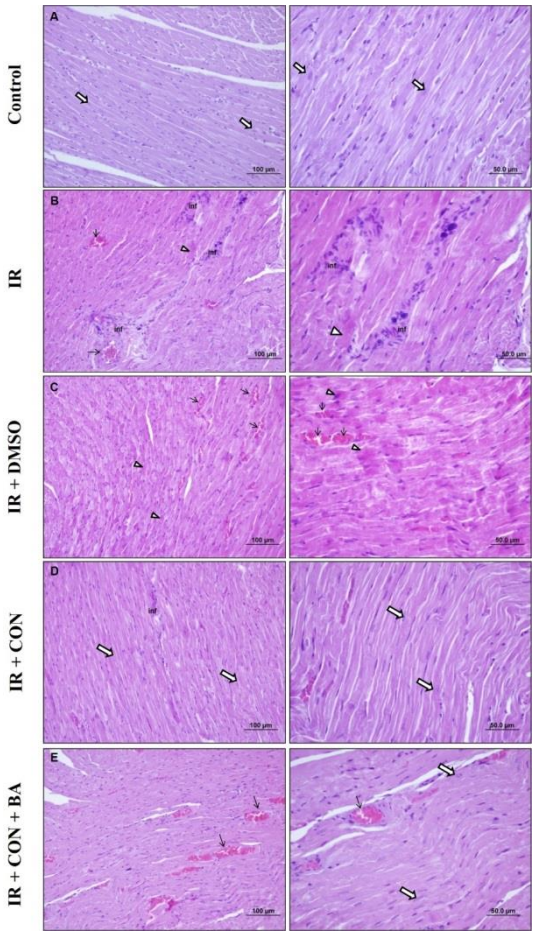

***Figure 6**. Representative images of rat heart sections. (A) Histologically normal muscle cells (⇨) with centrally located euchromatic nuclei in the control group. (B) Necrotic cells (▷) with pyknotic nuclei and eosinophilic cytoplasm, cellular inflammation (inf), and vascular congestion (→) in the connective tissue surrounding muscle fibers in heart tissue in the I/R group. (C) Necrotic cells (▷) with pyknotic nuclei and eosinophilic cytoplasm, and vascular congestion (→) in the connective tissue surrounding muscle fibers in the I/R+DMSO group. (D) Muscle cells in the I/R+CON group with minimal cellular inflammation (inf) and near-normal histologic structure of muscle cells with centrally located euchromatic nuclei (⇨). (E) In the I/R+CON+BA group, less damage compared to the I/R group, vascular congestion (→) in the connective tissue surrounding the muscle fibers, and muscle cells (⇨) with near-normal structure with centrally located euchromatic nuclei (Hematoxylin–eosin; scale bar: left to right 100µm, 50.0µm). I/R, ischemia-reperfusion; DMSO, dimethyl sulfoxide; CON, conivaptan; BA, boric acid.*

3.8. Pancreatic Tissue Histology

Upon microscopic examination of rat pancreatic tissue sections stained with HE, there was normal endocrine and exocrine pancreatic histology with islets of Langerhans and serous acinus structures in the control (Figure 7A) (Supplemental Table 3). In I/R group, acinar cell degeneration and vacuolization, intense edema in the intercellular space, inflammation, and vascular congestion were observed in pancreatic tissue (Figure 7B). In I/R+DMSO group, degeneration of the islet of Langerhans cells, acinar cells with pyknotic nuclei, and necrotic acinar structures were observed (Figure 7C). In I/R+CON group, the endocrine and exocrine pancreas structure had reduced damage and near-normal histologic structure with reference to I/R group (Figure 7D). Similar to I/R+CON treatment group, the I/R+CON+BA group had reduced damage compared to I/R group with histologically normal endocrine and exocrine pancreas structure (Figure 7E).

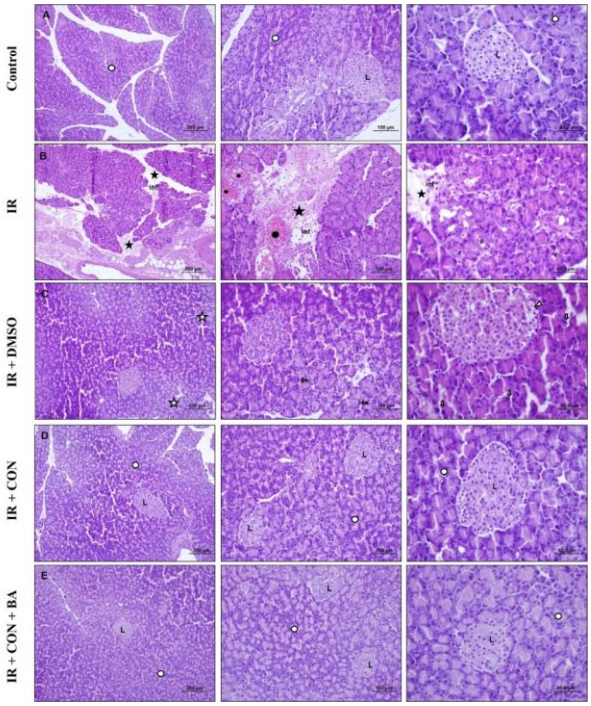

Figure 7. *Representative images of rat pancreatic sections. (A) Normal endocrine and exocrine pancreas histology with islets of Langerhans structure (L) and serous acinus structures (**o**) in the control group. (B) Acinar cell degeneration and vacuolization (v), intense edema (★), inflammation (inf), and vascular congestion (●) in the intercellular space in the I/R group. (C) Degeneration of islet cells of Langerhans (▷), acinar cells with pyknotic nuclei (⇨), and necrotic acinar structures (☆) in the I/R+DMSO group. (D) Reduced damage and near-normal endocrine (L: Islet of Langerhans) and exocrine pancreas structure (**o**) in the I/R+CON group compared to the I/R group. (E) Reduced damage and near-normal endocrine (L: Islet of Langerhans) and exocrine pancreas structure (**o**) in the I/R+CON+BA group compared to the I/R group (Hematoxylin–eosin; scale bar: left to right 200µm, 100µm, 50.0µm). I/R, ischemia-reperfusion; DMSO, dimethyl sulfoxide; CON, conivaptan; BA, boric acid.*

3.9. Testicular Tissue Histology

In the images of control group testicular tissue sections stained with HE, there were seminiferous tubule structures and spermatogenic cells in the tubule wall, spermatogenesis continuing in many tubules, interstitial space, and Leydig cells in normal structures (Figure 8A) (Supplemental Table 4). Atrophic tubule structures, tubular damage, cellular loss in the tubule wall, and vascular congestion in the interstitial area were observed in the testicular tissues of I/R group (Figure 8B). Similar to the I/R group, there were atrophic tubule structures, tubular damage, cellular loss in the tubule wall, and edema in the interstitial area in testicles of I/R+DMSO group (Figure 8C). In I/R+CON group, there was reduced damage with reference to I/R group and near-normal appearance of seminiferous tubules, spermatogenic cell series in the tubule wall, spermatogonium, primary spermatocytes, spermatids, Sertoli cells, and ongoing spermatogenesis in the tubules (Figure 8D). Spermatogenic cell lines, spermatogonium, primary spermatocytes, spermatids, and Sertoli cells with near-normal structure along with interstitial space and Leydig cells were observed in near-normal structure in testicles of I/R+CON+BA group rats (Figure 8E).

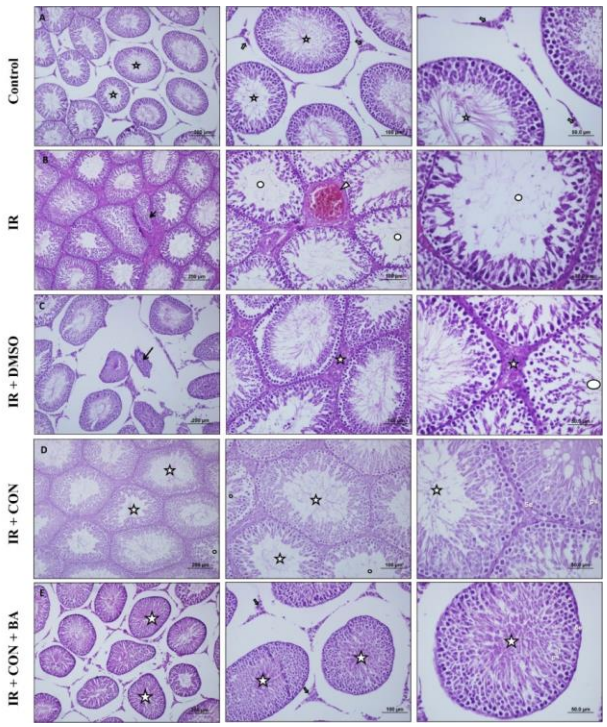

Figure 8. *Representative images of rat testicular sections. (A) In the testicles of the control group, the seminiferous tubule structures and spermatogenic cells in the tubule wall, ongoing spermatogenesis (★) in many tubules, interstitial space, and Leydig cells (⇨) were normal. (B) Atrophic tubule structures (→), tubular damage (o), cellular loss in the tubule wall, and vascular congestion in the interstitial space (►) in the I/R group. (C) Atrophic tubule structures (→), tubular damage (o), cellular loss in the tubule wall, and edema in the interstitial area (★) in the I/R+DMSO group. (D) In the I/R+CON group, there was reduced damage compared to the I/R group and near-normal appearance of seminiferous tubules (★), spermatogenic cell series in the tubule wall, spermatogonium (s), primary spermatocytes (ps), spermatids (st) and Sertoli cells (Se) and spermatogenesis continued in the tubules. (E) In the testicles of I/R+CON+BA group rats, reduced damage compared to the I/R group and near-normal appearance of seminiferous tubules (★), spermatogenic cell series in the tubule wall, spermatogonium (s), primary spermatocytes (ps), spermatids (st) and Sertoli cells (Se) and spermatogenesis continued in the tubules; interstitial space and Leydig cells (⇨) are in normal appearance (Hematoxylin–eosin; scale bar: left to right 200µm, 100µm, 50.0µm). I/R, ischemia-reperfusion; DMSO, dimethyl sulfoxide; CON, conivaptan; BA, boric acid.*

3.10. Spleen Tissue Histology

Rat spleen tissue sections stained with HE had normal-appearing cortex and parenchyma tissue in control group rats, along with white pulp, red pulp, and arteriole centralis were observed in normal histologic appearance (Figure 9A) (Supplemental Table 5). White pulp degeneration with parenchymal tissue damage was observed in spleens of I/R group rats, while the dense distribution of the red pulp region with reference to the white pulp was remarkable (Figure 9B). Similar to I/R group, there was white pulp degeneration with parenchymal tissue damage in I/R+DMSO group, with a dense distribution of the red pulp region with reference to the white pulp (Figure 9C). The cortex and parenchyma tissue were generally normal in I/R+CON group, although a few white pulp degenerations were observed in their spleens. White pulp, red pulp, and arteriole centralis were observed in a histologic appearance similar to the controls (Figure 9D). In I/R+CON+BA group, cortex and parenchyma tissues had a near-normal appearance, while white pulp, red pulp, and arteriole centralis were histologically similar to the controls (Figure 9E).

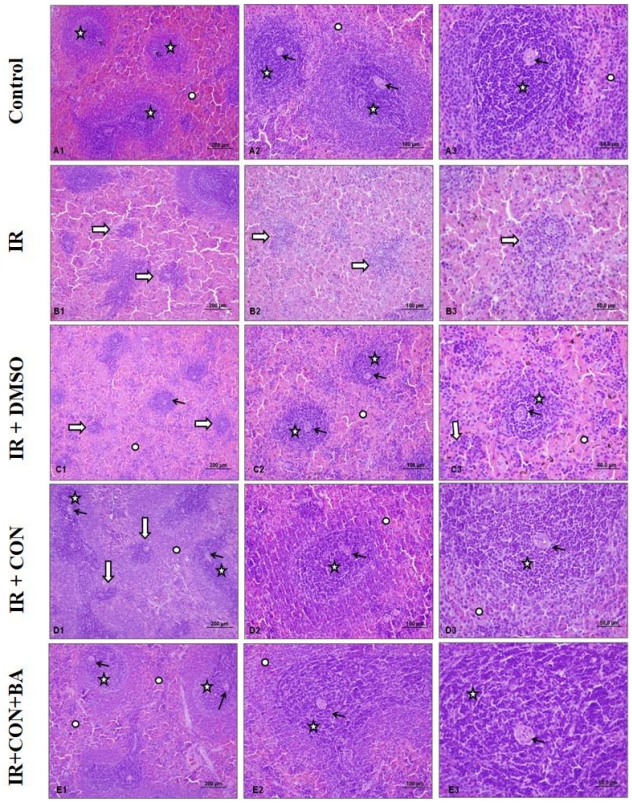

Figure 9. *Representative images of rat spleen sections. (A) Normal-appearing cortex and parenchymal tissue, white pulp (★), red pulp (o), and arteriole centralis (→) have histologically normal appearances in the control group. (B) White pulp degeneration (⇨) with parenchymal tissue damage in rat spleens of the I/R group, with a dense distribution of the red pulp region (o) compared to the white pulp (★). (C) White pulp degeneration (⇨) with parenchymal tissue damage in the I/R+DMSO group; dense distribution of the red pulp region (o) compared to the white pulp (★). (D) Although there is a little white pulp degeneration (⇨) in the spleens of the I/R+CON group, the cortex and parenchyma appear normal in general. White pulp (★), red pulp (o), and arteriole centralis (→) histologically similar to the controls (E) In the I/R+CON+BA group, cortex and parenchyma tissue appear close to normal; white pulp (★), red pulp (o), and arteriole centralis (→) histologically similar to the control (Hematoxylin–eosin; scale bar: left to right 200µm, 100µm, 50.0µm). I/R, ischemia-reperfusion; DMSO, dimethyl sulfoxide; CON, conivaptan; BA, boric acid.*

4. Discussion and Conclusion

Ischemia-reperfusion pathophysiology is a complicated process involving certain mechanisms, including metabolic alterations, free radical pathways, activation of immune reactions (46). Renal I/R injury can induce renal dysfunction by triggering mechanisms associated with oxidative stress and reactive oxygen/nitrogen species formation. A recent study considered that an individual investigation of antioxidant molecules to define the oxidative stress level might be limited to determine the total intracellular oxidant stress, so, TAS, TOS measurements, and OSI calculations might prove to be more accurate (47). Based on our results, TAS and TOS were significantly elevated in DMSO-treated I/R injury group with reference to control. Similarly, the TAS levels were elevated in treatment groups compared to control, and TOS levels significantly decreased with reference to the I/R injury group. Oxidative stress index values based on TAS and TOS levels were significantly lower in CON and BA treatment groups with reference to DMSO-treated I/R injury group. The study results associated with TAS, TOS, and OSI values supported the idea that CON alone and combined with BA was significantly effective against oxidative stress induced by renal I/R injury. It was remarkable that the oxidant level in systemic circulation decreased when BA was administered in combination with CON; this result may be considered an indicator of BA's antioxidant activity.

It was reported that ischemic damage might induce vasoconstriction and activate the inflammatory response; thus, ischemic tubular damage might turn into tubule necrosis and cause organ dysfunction (48, 49). It is well established that this inflammatory

response is related with an exacerbation of kidney damage (50). Systemic and local analysis of cytokine levels as proinflammatory/anti-inflammatory and/or immunomodulators has been widely preferred in investigating the inflammatory response to tissue damage. Tumor necrosis factor-alpha is a pleiotropic proinflammatory cytokine with various biological activities; it was suggested that TNF was produced by renal tubular epithelium and activated leukocytes and increased leukocyte infiltration because of I/R (51). Furthermore, it was reported that TNF induced the production of cytokines, including IL-6 and IL-10 (52). It was reported that IL-6, a proinflammatory cytokine, contributed to the progression of renal diseases at high concentrations, while at lower levels, it may have a role in the regulation of repair mechanisms (53). Interleukin-10 as a potent anti-inflammatory cytokine restricts inflammatory and cytotoxic processes involved in AKI and may be useful in preventing I/R injury (52, 54). Interleukin-35 was described as an adipocytokine with anti-inflammatory and immunosuppressive properties; interestingly, no studies investigated IL-35 levels in renal ischemia. Chemerin is a leukocyte chemoattractant (55) and a versatile protein serving important functions, including chemoattraction of innate immune cells as well as being widely expressed throughout tissues; furthermore, there is also evidence that chemerin is an adipocytokine (56). Besides, recent studies investigated circulating chemerin levels and their pathophysiological significance in chronic kidney disease populations; although it was emphasized that there were still gaps, especially as to whether elevated chemerin levels were the cause or reflection of decreased renal function, it was considered that measurement of chemerin serum levels would provide important information about its role in pathophysiology of several diseases and whether it was a diagnostic/therapeutic marker (57). In our study, serum cytokine levels and their mRNA expressions in kidney tissue were analysed. Based on the results of serum samples, proinflammatory TNF-α was elevated in DMSO-treated I/R group with reference to control group. Although serum TNF-α levels tended to decrease, there was no crucial difference between the treatment groups. Serum IL-10 levels were observed to increase in I/R injury group treated with DMSO with reference to the control, while the highest values were observed in CON treatment group. Although there were no significant intergroup differences in IL-6, IL-35, and chemerin levels, there was an evident tendency to increase in IL-35 and chemerin levels in treatment groups. In line with these results, I/R injury increased proinflammatory and anti-inflammatory cytokine levels. It may be suggested that CON treatment played an active role in the pro-/anti-inflammatory cytokine balance against injury by tending to increase IL-10, IL-35, and chemerin in circulation during the early damage period. This effect was not observed to this extent in combination treatment with BA. In addition to serum analysis, mRNA expression analysis of kidney tissue indicated that TNF-α, IL-6, IL-10, and chemerin mRNA expressions increased in I/R injury groups with reference to controls. In contrast, proinflammatory TNF-α and IL-6 and anti-inflammatory IL-10 and chemerin expression levels were significantly decreased in both treatment groups compared to I/R injury groups. Similar to the serum cytokine results, I/R injury also increased proinflammatory and anti-inflammatory cytokine levels at the renal tissue level, suggesting that the I/R process might trigger inflammatory processes and cause renal dysfunction. It was concluded that CON and BA treatments reduced the expression levels of all these proinflammatory and anti-inflammatory proteins to low values close to the control group in general and helped maintain the pro-/anti-inflammatory cytokine balance in kidney.

The present study investigated the efficacy of BA and CON on liver damage as a remote tissue. Upon analyses of liver function tests (serum enzyme activities, albumin levels) and lipid profile (serum total/LDL/HDL-cholesterol and triglyceride levels), serum ALT, AST, and ALP activities tended to increase in the early period in the I/R group with reference to control. Albumin levels decreased in DMSO-treated I/R injury group; a tendency to decrease was also observed in treatment groups, but there was no statistical difference. This may be associated with albumin being a rapidly regenerating serum protein. In liver histology, hepatocytes with pyknotic nuclei observed in the parenchymal tissue, necrotic areas in the periportal region, intravenular congestion, edema, and inflammation findings in the portal area were indicative of the fact that tissue damage began to occur in the early period. There were no significant differences in ALT, AST, and ALP activities in treatment groups, and histologic findings of the study, including minimal degeneration, reduced damage, and near-normal liver structure, supported these biochemical findings. Upon analysis of the lipid profile, CON treatment decreased LDL-cholesterol levels, while combined treatment with BA significantly increased with reference to I/R group. Histologic images of the combination therapy group did not show any evidence of exacerbation of damage with reference to CON group. Nevertheless, there were high HDL-cholesterol and low triglyceride levels in combination therapy group, suggesting that the combination therapy might effectively control liver

damage and protect hepatic lipid metabolism. Furthermore, the fact that there were no signs of edema in the tissue in treatment groups upon histological analysis suggests that CON prevents and/or delays the formation of edema in the early period thanks to its aquaretic effect.

In addition to liver as a distant tissue, heart, pancreas, testis, and spleen tissues of rats as distant organs were also investigated. These tissues were stained with HE, followed by histological evaluations of the general condition of the tissues. Based on the histologic findings of the study, in general, very close results were obtained between I/R and DMSO-treated I/R injury groups and between both treatment groups. As a result, renal I/R can induce necrosis, inflammation, and functional tissue damage, leading to significant distant organ damage even in the early period; furthermore, the combination therapies with a single dose of 10 mg/kg CON (i.v.) and a single dose of 50 mg/kg BA (i.p.) at the onset of reperfusion may reduce, prevent, and/or delay damage to distant organs of liver, heart, pancreas, testis and spleen during the postischemic period.

In briefly, this study demonstrated that CON, alone or in combination with BA, exerts protective effects against renal I/R injury in a rat model with contralateral nephrectomy. The study focused on the acute period, and a general account of the results is as follows: 1) It was demonstrated that renal ischemia in rats could trigger oxidative stress and inflammation, causing significant functional and/or structural alterations related with damage to the kidney, as well as distant tissues such as liver, heart, pancreas, testis, and spleen. 2) The results of I/R and I/R+DMSO groups were biochemically and histologically similar; therefore, DMSO used as a solvent was not associated with an increasing effect on the damage during the postischemic process. 3) Conivaptan, especially when administered in combination with BA, improved hepatic lipid metabolism. 4) Boric acid might be more effective on oxidative stress when applied in combination with CON. 5) Histologic analyses showed generally no signs of edema (or rarely mild edema) in tissues of treatment groups, which suggested that CON prevented/delayed edema occurrence by its aquaretic effect. These findings suggest that CON, with or without BA, may offer therapeutic value in mitigating the acute effects of renal I/R injury and its systemic consequences.

In conclusion, our findings suggest that CON and BA possess complementary antioxidant and anti-inflammatory properties that mitigate renal and distant organ injury in the early phase of I/R. So far, no experimental or clinical data in this context have been reported in the relevant literature. This study was limited to acute-phase observations and did not assess long-term outcomes. Additionally, pharmacokinetic data, repeated-dose effects, and cross-species efficacy were not explored. Future studies should address these aspects to better define the potential of CON and BA in renal I/R injury management.

REFERENCES

1. KDIGO clinical practice guideline for acute kidney injury. Chapter 21: definition and classification of AKI. Kidney Int, 2012; 2(Suppl 1): p. 19–22.
2. Hoste, E.A.J., Kellum, J.A., Selby, N.M., Zarbock, A., Palevsky, P.M., Bagshaw, S.M., Goldstein, S.L., Cerdá, J., Chawla, L.S. Global epidemiology and outcomes of acute kidney injury. Nat Rev Nephrol, 2018. 14(10): p. 607–625.
3. Ronco, C., Bellomo, R., Kellum, J.A. Acute kidney injury. Lancet, 2019. 394(10212): p. 1949–1964.
4. Hoste, E.A., Bagshaw, S.M., Bellomo, R., Cely, C.M., Colman, R., Cruz, D.N., Edipidis, K., Forni L.G., Gomersall, C.D., Govil, D., Honoré, P.M., Joannes-Boyau, O., Joannidis, M., Korhonen, A.M., Lavrentieva, A., Mehta, R.L., Palevsky P., Roessler, E., Ronco, C., Uchino, S., Vazquez, J.A., Vidal Andrade, E., Webb, S., Kellum, J.A. Epidemiology of acute kidney injury in critically ill patients: the multinational AKI-EPI study. Intensive Care Med, 2015. 41(8): p. 1411–1423.
5. Li, N., Wang, Y., Wang, X., Sun, N., Gong, Y.H. Pathway network of pyroptosis and its potential inhibitors in acute kidney injury. Pharmacol Res, 2022. 175:106033.
6. White, L.E., Hassoun, H.T. Inflammatory mechanisms of organ crosstalk during ischemic acute kidney injury. Int J Nephrol, 2012. 505197.
7. Abogresha, N.M., Greish, S.M., Abdelaziz, E.Z., Khalil, W.F. Remote effect of kidney ischemia-reperfusion injury on pancreas: role of oxidative stress and mitochondrial apoptosis. Arch Med Sci, 2016. 12(2): p. 252–262.
8. Jang, H.R., Rabb, H. Immune cells in experimental acute kidney injury. Nat Rev Nephrol, 2015. 11(2): p. 88–101.
9. Yang, L., Besschetnova, T.Y., Brooks, C.R., Shah, J.V., Bonventre, J.V. Epithelial cell cycle arrest in G2/M mediates kidney fibrosis after injury. Nat Med, 2010. 16(5): p. 535–543.
10. Fu, Y., Tang, C., Cai, J., Chen, G., Zhang, D., Dong, Z. Rodent models of AKI-CKD transition. Am J Physiol Renal Physiol, 2018. 315(4): F1098–F1106.
11. Finn, W.F., Fernandez-Repollet, E., Goldfarb, D., Iaina, A., Eliahou, H.E. Attenuation of injury due to

unilateral renal ischemia: delayed effects of contralateral nephrectomy. J Lab Clin Med, 1984. 103(2): p. 193–203.
12. Owji, S.M., Nikeghbal, E., Moosavi, S.M. Comparison of ischaemia-reperfusion-induced acute kidney injury by clamping renal arteries, veins or pedicles in anaesthetized rats. Exp Physiol, 2018. 103(10): p. 1390–1402.
13. Shiva, N., Sharma, N., Kulkarni, Y.A., Mulay, S.R., Gaikwad, A.B. Renal ischemia/reperfusion injury: an insight on in vitro and in vivo models. Life Sci, 2020; 256: 117860.
14. Senturk, H., Kabay, S., Bayramoglu, G., Ozden, H., Yaylak, F., Yucel, M., Olgun, E.G., Kutlu, A. Silymarin attenuates the renal ischemia/reperfusion injury-induced morphological changes in the rat kidney. World J Urol, 2008. 26(4): p. 401–407.
15. Can, B., Kar, F., Kar, E., Özkoç, M., Şentürk, H., Dönmez, D.B., Kanbak, G., Alataş, İ.Ö. Conivaptan and boric acid treatments in acute kidney injury: is this combination effective and safe?. Biol Trace Elem Res, 2022. 200(8): p. 3723–3737.
16. Meijer, E., Boertien, W.E., Zietse, R., Gansevoort, R.T. Potential deleterious effects of vasopressin in chronic kidney disease and particularly autosomal dominant polycystic kidney disease. Kidney Blood Press Res, 2011. 34(4): p. 235–244.
17. Moen, M.D., Keating, G.M. Intravenous conivaptan. Am J Cardiovasc Drugs, 2008. 8(5): p. 341–348.
18. Palmer, B.F. Vasopressin receptor antagonists. Curr Hypertens Rep, 2015. 17(1): p. 510.
19. Ferguson-Myrthil, N. Novel agents for the treatment of hyponatremia: a review of conivaptan and tolvaptan. Cardiol Rev, 2010. 18(6): p. 313–321.
20. García-Arroyo, F.E., Tapia, E., Blas-Marron, M.G., Gonzaga, G., Silverio, O., Cristóbal, M., Osorio, H., Arellano-Buendía, A.S., Zazueta, C., Aparicio-Trejo, O.E., Reyes-García, J.G., Pedraza-Chaverri, J., Soto, V., Roncal-Jiménez, C., Johnson, R.J., Sánchez-Lozada, L.G. Vasopressin mediates the renal damage induced by limited fructose rehydration in recurrently dehydrated rats. Int J Biol Sci, 2017. 13(8): p. 961–975.
21. Cabus, U., Secme, M., Kabukcu, C., Cil, N., Dodurga, Y., Mete, G., Fenkci, I.V. Boric acid as a promising agent in the treatment of ovarian cancer: molecular mechanisms. Gene, 2021. 796–797: 145799.
22. Union of Turkish chambers of mechanical engineers and architects (UCTEA). (TMMOB in Turkish). The Boron Report. May, 2016. (http://www.tmmob.org.tr). ISBN: 978-605-01-0883-5.
23. Colak, S., Geyikoglu, F., Keles, O.N., Türkez, H., Topal, A., Unal B. The neuroprotective role of boric acid on aluminum chloride-induced neurotoxicity. Toxicol Ind Health, 2011. 27(8): p. 700–710.
24. Ince, S., Keles, H., Erdogan, M., Hazman, O., Kucukkurt, I. Protective effect of boric acid against carbon tetrachloride-induced hepatotoxicity in mice. Drug Chem Toxicol, 2012. 35(3): p. 285–292.
25. Scorei, R., Ciubar, R., Ciofrangeanu, C.M., Mitran, V., Cimpean, A., Iordachescu, D. Comparative effects of boric acid and calcium fructoborate on breast cancer cells. Biol Trace Elem Res, 2008. 122(3): p. 197–205.
26. Rajendran, K.G., Chen, S.Y., Sood, A., Spielvogel, B.F., Hall, I.H. The anti-osteoporotic activity of amine-carboxyboranes in rodents. Biomed Pharmacother, 1995. 49(3): p. 131–140.
27. Chen, Z., Wu, H., Wang, H., Zaldivar-Silva, D., Agüero, L., Liu, Y., Zhang, Z., Yin, Y., Qiu, B., Zhao, J., Lu, X., Wang, S. An injectable anti-microbial and adhesive hydrogel for the effective noncompressible visceral hemostasis and wound repair. Mater Sci Eng C Mater Biol Appl, 2021. 129: 112422.
28. Cetiner, E., Sayin, K., Tuzun, B., Ataseven, H. Could boron-containing compounds (BCCs) be effective against SARS-CoV-2 as anti-viral agent? Bratisl Lek Listy, 2021. 122(4): p. 263–269.
29. Sogut, I., Oglakci, A., Kartkaya, K., Ol, K.K., Sogut, M.S., Kanbak, G., Inal, M.E. Effect of boric acid on oxidative stress in rats with fetal alcohol syndrome. Exp Ther Med, 2015. 9(3): p. 1023–1027.
30. Ataizi, Z.S., Ozkoc, M., Kanbak, G., Karimkhani, H., Burukoglu Donmez, D., Ustunisik, N., Ozturk, B. Evaluation of the Neuroprotective Role of Boric Acid in Preventing Traumatic Brain Injury-Mediated Oxidative Stress. Turk Neurosurg, 2021. 31(4): p. 493-499.
31. Hacioglu, C., Kar, F., Kacar, S., Sahinturk, V., Kanbak, G. High concentrations of boric acid trigger concentration-dependent oxidative stress, apoptotic pathways and morphological alterations in DU-145 human prostate cancer cell line. Biol Trace Elem Res, 2020. 193(2): p. 400–409.
32. Karimkhani, H., Özkoç, M., Shojaolsadati, P., Uzuner, K., Donmez, D.B., Kanbak, G. Protective effect of boric acid and omega-3 on myocardial ınfarction in an experimental rat model. Biol Trace Elem Res, 2021. 199(7): p. 2612–2620.
33. Özkoç, M., Can, B., Şentürk, H., Burukoğlu Dönmez, D., Kanbak, G. Possible curative effects of boric acid and bacillus clausii treatments on TNBS-ınduced ulcerative colitis in rats. Biol Trace Elem Res, 2023. 201(3): p. 1237–1251.
34. İlhan, A.O, Can, B., Kar, F., Gündoğdu, A.Ç., Söğüt, İ., Kanbak, G. An investigation into the protective effects of various doses of boric acid on liver, kidney, and brain tissue damage caused by high levels of acute alcohol consumption Biol Trace Elem Res, 2023. 201(11): p. 5346–5357.
35. Lopalco, A., Lopedota, A.A., Laquintana, V., Denora, N., Stella, V.J. Boric acid, a lewis acid with unique and unusual properties: formulation ımplications. J Pharm Sci, 2020. 109(8): p. 2375–2386.
36. Karim, M., Boikess, R.S., Schwartz, R.A., Cohen, P.J. Dimethyl sulfoxide (DMSO): a solvent that may solve selected cutaneous clinical challenges. Arch Dermatol Res., 2023. 315(6): p. 1465-1472.
37. Roldán-Fidalgo, A., Trinidad, A., Rodríguez-Valiente, A., García-Berrocal, J.R., Millán, I., Coronado, M.J., Ramírez-Camacho, R. Effect of intratympanic dimethyl sulphoxide (DMSO) in an in vivo model of cisplatin-related ototoxicity. Eur Arch Otorhinolaryngol, 2014. 271(12): p. 3121-6.
38. Can, B., Oz, S., Sahinturk, V., Musmul, A., Alatas, İ.O. Effects of conivaptan versus mannitol on post-ischemic brain injury and edema. Eurasian J Med, 2019. 51(1): p. 42–48.
39. Kar, F., Hacioglu, C., Senturk, H., Donmez, D.B., Kanbak G. The role of oxidative stress, renal ınflammation, and apoptosis in post ıschemic reperfusion ınjury of kidney tissue: the protective

effect of dose-dependent boric acid administration. Biol Trace Elem Res, 2020. 195(1): p. 150–158.
40. Bolukbas, C., Bolukbas, F.F., Horoz, M., Aslan, M., Celik, H., Erel, O. Increased oxidative stress associated with the severity of the liver disease in various forms of hepatitis B virus infection. BMC Infect Dis, 2005. 5:95.
41. Azouz, A. A., Hersi, F., Ali, F. E. M., Hussein Elkelawy, A. M. M., Omar, H. A. Renoprotective effect of vinpocetine against ischemia/reperfusion injury: Modulation of NADPH oxidase/Nrf2, IKKβ/NF-κB p65, and cleaved caspase-3 expressions. Journal of biochemical and molecular toxicology, 2022. 36(7): e23046.
42. Zhang, C., Sun, B., Wang, L., Korla, P. K., Liu, C. Micheliolide mitigates diabetic nephropathy by modulating oxidative stress and inflammation in rats. Phytomedicine: international journal of phytotherapy and phytopharmacology, 2025. 145: 157025.
43. Raza, S. M., Mehmood, M. H., Mehdi, S., Saadullah, M., Faisal, M. N. Distachionate and Its Nanocomposites Modulate Oxidative Stress, Inflammation, and Diabetes-Related Genes in High-Fructose/Streptozotocin Model. ACS omega, 2025. 10(30): p. 33353–33370.
44. Livak, K. J., Schmittgen, T. D. Analysis of relative gene expression data using real-time quantitative PCR and the 2(-Delta Delta C(T)) Method. Methods (San Diego, Calif.), 2001. 25(4): p. 402–408.
45. Sahin, S., Burukoglu Donmez, D. Effects of Carnosine (Beta-Alanyl-L-Histidine) in an Experimental Rat Model of Acute Kidney Injury Due to Septic Shock. Medical science monitor: international medical journal of experimental and clinical research, 2018. 24: p. 305–316.
46. Varga, G., Ghanem, S., Szabo, B., Nagy, K., Pal, N., Tanczos, B., Somogyi, V., Barath, B., Deak, A., Peto, K., Nemeth, N. Renal ischemia-reperfusion-induced metabolic and micro-rheological alterations and their modulation by remote organ ischemic preconditioning protocols in the rat. Clin Hemorheol Microcirc, 2019. 71(2): p. 225-236.
47. Acar, M., Sayhan Kaplan, H., Erdem, A.F., Tomak, Y., Turan, G., Özdin, M. Effects of dexmedetomidine on new oxidative stress markers on renal ischaemia-reperfusion injury in rats: thiol/disulphide homeostasis and the ischaemia-modified albumin. Arch Physiol Biochem, 2022. 128(4): p. 1115–1120.
48. Farrar, A. Acute kidney injury. The Nursing clinics of North America, 2018. 53(4): p. 499–510.
49. Sluman, C., Gudka, P.M., McCormick, K. Acute kidney injury: pre-renal, intra-renal and post-renal. In: Braund R. editor. Renal medicine and clinical pharmacy. Advanced clinical pharmacy-research, development and practical applications, 2020. Vol. 1. Springer, Cham.
50. Zuk, A., Bonventre, J.V. Acute kidney injury. Annu Rev Med, 2016. 67: p. 293–307.
51. Domínguez Fernández, E., Siemers, F., Flohé, S., Nau, M., Schade, F.U. Effects of endotoxin tolerance on liver function after hepatic ischemia/reperfusion injury in the rat. Crit Care Med, 2002. 30(1): p. 165–170.
52. Godet, C., Goujon J.M., Petit I., Lecron J.C., Hauet T., Mauco G., Carretier M., Robert, R. Endotoxin tolerance enhances interleukin-10 renal expression and decreases ischemia-reperfusion renal injury in rats. Shock (Augusta, Ga.), 2006. 25(4): p. 384–388.
53. Kayama, F., Yoshida, T., Kodama, Y., Matsui, T., Matheson, J.M., Luster, M.I. Pro-inflammatory cytokines and interleukin 6 in the renal response to bacterial endotoxin. Cytokine, 1997. 9(9): p. 688–695.
54. Deng, J., Kohda, Y., Chiao, H., Wang, Y., Hu, X., Hewitt, S.M., Miyaji, T., McLeroy, P., Nibhanupudy, B., Li, S., Star, R.A. Interleukin-10 inhibits ischemic and cisplatin-induced acute renal injury. Kidney Int, 2001. 60(6): p. 2118–2128.
55. Nagpal, S., Patel, S., Jacobe, H., DiSepio, D., Ghosn, C., Malhotra, M., Teng, M., Duvic, M., Chandraratna, R.A. Tazarotene-induced gene 2 (TIG2), a novel retinoid-responsive gene in skin. J Invest Dermatol, 1997. 109(1): p. 91–95.
56. Goralski, K.B., McCarthy, T.C., Hanniman, E.A., Zabel, B.A., Butcher, E.C., Parlee, S.D., Muruganandan, S., Sinal, C.J. Chemerin, a novel adipokine that regulates adipogenesis and adipocyte metabolism. J Biol Chem, 2007. 282(38): p. 28175–28188.
57. Bonomini, M., Pandolfi, A. Chemerin in renal dysfunction and cardiovascular disease. Vascul Pharmacol, 2016. 77: p. 28–34.